REPORT DOCUMENTATION PAGE

Form Approved OMB NO. 0704-0188

1. REPORT DATE (DD-MM-YYYY)	2. REPORT TYPE	3. DATES COVERED (From - To)
30-03-2012	Book	-

4. TITLE AND SUBTITLE
Orbital evasive target tracking and sensor management

5a. CONTRACT NUMBER
W911NF-08-1-0409

5b. GRANT NUMBER

5c. PROGRAM ELEMENT NUMBER
611102

6. AUTHORS
G. Chen, D. Shen, E. Blasch, K. Pham, H. Chen

5d. PROJECT NUMBER

5e. TASK NUMBER

5f. WORK UNIT NUMBER

7. PERFORMING ORGANIZATION NAMES AND ADDRESSES
University of New Orleans
2000 Lakeshore Drive

New Orleans, LA 70148 -

8. PERFORMING ORGANIZATION REPORT NUMBER

9. SPONSORING/MONITORING AGENCY NAME(S) AND ADDRESS(ES)
U.S. Army Research Office
P.O. Box 12211
Research Triangle Park, NC 27709-2211

10. SPONSOR/MONITOR'S ACRONYM(S)
ARO

11. SPONSOR/MONITOR'S REPORT NUMBER(S)
54370-CS.80

12. DISTRIBUTION AVAILIBILITY STATEMENT
Approved for public release; distribution is unlimited.

13. SUPPLEMENTARY NOTES
The views, opinions and/or findings contained in this report are those of the author(s) and should not contrued as an official Department of the Army position, policy or decision, unless so designated by other documentation.

14. ABSTRACT
In this chapter, we consider the sensor management problem for tracking space targets where the targets may apply evasive maneuvering strategy to avoid being tracked by the space borne observers. We first study the case of single target tracking by a single observer and formulate the pursuit–evasion game with complete information. Then we extend the tracking problem to a set of collaborative observers

15. SUBJECT TERMS
a,b,c,d,e

16. SECURITY CLASSIFICATION OF:			17. LIMITATION OF ABSTRACT	15. NUMBER OF PAGES	19a. NAME OF RESPONSIBLE PERSON
a. REPORT	b. ABSTRACT	c. THIS PAGE			X. Rong Li
UU	UU	UU	UU		19b. TELEPHONE NUMBER: 504-280-7416

Report Title

Orbital evasive target tracking and sensor management

ABSTRACT

In this chapter, we consider the sensor management problem for tracking space targets where the targets may apply evasive maneuvering strategy to avoid being tracked by the space borne observers. We first study the case of single target tracking by a single observer and formulate the pursuit–evasion game with complete information. Then we extend the tracking problem to a set of collaborative observers and each observer has to decide when to sense which target in order to achieve the desired estimation error covariance. A popularly used criterion for sensor management is to maximize the total information gain in the observer-to-target assignment. We compare the information based approach to the game theoretic criterion where the observers are assigned according to the best response of the terminal result in the pursuit–evasion game. Finally, we use realistic satellite orbits to simulate the space resource management for situation awareness. We adopted NASA's General Mission Analysis Tool (GMAT) for space target tracking with multiple space borne observers. The results indicate that the game theoretic approach is more effective than the information based approach in handling intelligent target maneuvers.

Chapter 12
Orbital Evasive Target Tracking and Sensor Management

**Huimin Chen, Genshe Chen, Dan Shen,
Erik P. Blasch, and Khanh Pham**

Summary In this chapter, we consider the sensor management problem for tracking space targets where the targets may apply evasive maneuvering strategy to avoid being tracked by the space borne observers. We first study the case of single target tracking by a single observer and formulate the pursuit–evasion game with complete information. Then we extend the tracking problem to a set of collaborative observers and each observer has to decide when to sense which target in order to achieve the desired estimation error covariance. A popularly used criterion for sensor management is to maximize the total information gain in the observer-to-target assignment. We compare the information based approach to the game theoretic criterion where the observers are assigned according to the best response of the terminal result in the pursuit–evasion game. Finally, we use realistic satellite orbits to simulate the space resource management for situation awareness. We adopted NASA's General Mission Analysis Tool (GMAT) for space target tracking with multiple space borne observers. The results indicate that the game theoretic approach is more effective than the information based approach in handling intelligent target maneuvers.

12.1 Introduction

Over recent decades, the space environment has become more complex with a significant increase in space debris among densely populated satellites. Efficient and

H. Chen
Department of Electrical Engineering, University of New Orleans, New Orleans, LA, USA

G. Chen (✉) · D. Shen
DCM Research Resources, LLC, Germantown, MD, USA
e-mail: gchen@dcmresearchresources.com

E.P. Blasch
AFRL/RYAA, WPAFB, OH, USA

K. Pham
AFRL/RVSV, Kirtland AFB, NM, USA

M.J. Hirsch et al. (eds.), *Dynamics of Information Systems,*
Springer Optimization and Its Applications 40, DOI 10.1007/978-1-4419-5689-7_12,

reliable space operations rely heavily on the space situation awareness where search and tracking space targets and identifying their intent are crucial in creating a consistent global picture of the space. Orbit determination with measurements provided by a constellation of satellites has been studied extensively [6, 7, 14, 16]. The tracking and data relay satellite system uses satellites in geostationary orbits (GEO) to track the satellites in low-Earth orbit (LEO). The global positioning system (GPS) uses a constellation of satellites with pseudo-range measurements, i.e., range measurements with clock differentials to determine the location of a user. Unlike ground targets whose motion may contain frequent maneuvers, a satellite usually follows its orbit so that long-term prediction of its orbital trajectory is possible once the orbital elements are known [6]. However, a space target can also make an orbital change owing to its desired mission or intentionally hiding from the space borne observers. Existing maneuvering target tracking literature mainly focuses on modeling target maneuver motion at random onset time (see, e.g., [1, 13]). In space surveillance, the constellation of satellite observers is usually known to the adversary and very unlikely to change frequently due to energy constraint. In this case, evasive maneuvering motion can be intelligently designed to take advantage of the sensing geometry, e.g., transferring to an orbit with maximum duration of the Earth blockage to an observer with known orbital trajectory. Accordingly, a sensor management method has to optimally utilize the sensing resources to acquire and track space targets with sparse measurements, i.e., with a typically large sampling interval, in order to maintain a large number of tracks simultaneously.

Sensor management is concerned with the sensor-to-target assignment and a schedule of sensing actions for each sensor in the near future given the currently available information on the space targets. Sensor assignment and scheduling usually aim to optimize a certain criterion under energy, data processing and communication constraints. One popularly used criterion is the total information gain for all the targets being tracked [11]. However, this criterion does not prioritize the targets with respect to their types or identities. Alternatively, covariance control optimizes the sensing resources to achieve the desired estimation error covariance for each target [10]. It has the flexibility to design the desired tracking accuracy according to the importance of each target. We want to compare both informative based criterion and the covariance control method in a game theoretic setting where the target can intelligently choose its maneuvering motion and onset time based on the knowledge of observers' constellation.

The rest of the chapter is organized as follows. Section 12.2 presents the space target motion and sensor measurement model. Section 12.3 provides a game theoretic formulation of target maneuvering motion. Section 12.4 discusses the information based performance metric for sensor management and covariance control method with possibly evasive target maneuvering motion. Section 12.5 compares the performance of the proposed tracking and sensor management scheme with the existing methods. Conclusions and future work are presented in Sect. 12.6.

12.2 Fundamentals of Space Target Orbits

12.2.1 Time and Coordinate Systems

Several time systems are popularly used in the orbit determination problems. Satellite laser ranging measurements are usually time-tagged in coordinated universal time (UTC) while global positioning system (GPS) measurements are time tagged in GPS system time (GPS-ST). Although both UTC and GPS-ST are based on atomic time standards, UTC is loosely tied to the rotation of the Earth through the application of "leap seconds" while GPS-ST is continuous with the relation GPS-ST = UTC + n where n is the number of leap seconds since January 6, 1980. The orbital equation describing near-Earth satellite motion is typically tagged with terrestrial dynamical time (TDT). It is an abstract, uniform time scale implicitly defined by the motion equation and can be converted to UTC or GPS-ST for any given reference date.

The Earth centered inertial (ECI) coordinate system used to link GPS-ST with UTC is a geocentric system defined by the mean equator and vernal equinox at Julian epoch 2000.0. Its XY-plane coincides with the equatorial plane of the Earth and the X-axis points toward the vernal equinox direction. The Z-axis points toward the north pole and the Y-axis completes the right hand coordinate systems.

The Earth centered Earth fixed (ECEF) coordinate system has the same XY-plane and the Z-axis as in the inertial coordinate system. However, its X-axis rotates with the Earth and points to the prime meridian and the Y-axis completes the right hand coordinate systems.

The local Cartesian system commonly referred to as east-north-up (ENU) coordinate system has its origin at some point on the Earth surface or above (typically at the location of an observer). Its Z-axis is normal to the Earth's reference ellipsoid defined by the geodetic latitude. The X-axis points toward the east while the Y-axis points toward the north. The conversion among these three coordinate systems is provided in Appendix 1.

12.2.2 Orbital Equation and Orbital Parameter Estimation

Without any perturbing force, the position $\mathbf{r}$ of a space target relative to the center of the Earth in ECI coordinate system should satisfy

$$\ddot{\mathbf{r}} = -\frac{\mu}{\|\mathbf{r}\|^3}\mathbf{r} \tag{12.1}$$

where μ is the Earth's gravitational parameter. The target velocity is $\mathbf{v} \triangleq \dot{\mathbf{r}}$ and the radial velocity is $v_r \triangleq \frac{\mathbf{v}\cdot\mathbf{r}}{r}$ where $r \triangleq \|\mathbf{r}\|$ is the distance from the target to the center of the Earth. In order to determine the position and velocity of a satellite at any time instance, six parameters are needed, typically, the three position components

and three velocity components at a certain time instance. Alternatively, the orbital trajectory can be conveniently described by the six components of the Keplerian elements. The description of Keplerian elements and their relationship to the kinematic state of the target can be found in Appendix 2.

In reality, a number of forces act on the satellite in addition to the Earth's gravity. To distinguish them from the central force created by the satellite target, these forces are often referred to as perturbing forces. In a continuous time state space model, perturbing forces are often lumped into the noise term of the system dynamics. Denote by $\mathbf{x}(t)$ the continuous time target state given by

$$\mathbf{x}(t) \triangleq \begin{bmatrix} \mathbf{r}(t) \\ \dot{\mathbf{r}}(t) \end{bmatrix} = \begin{bmatrix} x(t) \\ y(t) \\ z(t) \\ v_x(t) \\ v_y(t) \\ v_z(t) \end{bmatrix} \tag{12.2}$$

For convenience, we omit the argument t and write the nonlinear state equation as follows.

$$\dot{\mathbf{x}} = f(\mathbf{x}) + \mathbf{w} \tag{12.3}$$

where

$$f(\mathbf{x}) = \begin{bmatrix} v_x \\ v_y \\ v_z \\ -(\mu/r^3)x \\ -(\mu/r^3)y \\ -(\mu/r^3)z \end{bmatrix} \tag{12.4}$$

and

$$\mathbf{w} = \begin{bmatrix} 0 \\ 0 \\ 0 \\ w_x \\ w_y \\ w_z \end{bmatrix} \tag{12.5}$$

is the acceleration resulting from perturbing forces. As opposed to treating the perturbing acceleration as noise, spacecraft general propagation (SGP) model maintains general perturbation element sets and finds analytical solution to the satellite motion equation with time varying Keplerian elements [12]. For precise orbit determination, numerical integration of (12.3) is often a viable solution where both the epoch state and the force model have to be periodically updated when a new measurement is available [17].

12.3 Modeling Maneuvering Target Motion in Space Target Tracking

12.3.1 Sensor Measurement Model

We consider the case that a space satellite in low-Earth orbit (LEO) observes a target in geostationary orbit (GEO). A radar onboard the space satellite can provide the following type of measurements: range, azimuth, elevation, and range rate. The range between the ith observer located at (x_i, y_i, z_i) and the space target located at (x, y, z) is given by

$$d_r(i) = \sqrt{(x - x_i)^2 + (y - y_i)^2 + (z - z_i)^2} \tag{12.6}$$

The azimuth is

$$d_a(i) = \tan^{-1}\left(\frac{y - y_i}{x - x_i}\right) \tag{12.7}$$

The elevation is

$$d_e(i) = \tan^{-1}\left(\frac{z - z_i}{\sqrt{(x - x_i)^2 + (y - y_i)^2}}\right) \tag{12.8}$$

The range rate is

$$d_{\dot{r}}(i) = \frac{(x - x_i)(\dot{x} - \dot{x}_i) + (y - y_i)(\dot{y} - \dot{y}_i) + (z - z_i)(\dot{z} - \dot{z}_i)}{d_r} \tag{12.9}$$

Measurements from the ith observer will be unavailable when the line-of-sight path between the observer and the target is blocked by the Earth. Thus, the constellation of multiple observers is important to maintain consistent coverage of the target of interest.

The condition of Earth blockage is examined as follows. If there exist $\alpha \in [0, 1]$ such that $D_\alpha(i) < R_E$, where

$$D_\alpha(i) = \sqrt{\left[(1 - \alpha)x_i + \alpha x\right]^2 + \left[(1 - \alpha)y_i + \alpha y\right]^2 + \left[(1 - \alpha)z_i + \alpha z\right]^2} \tag{12.10}$$

then the measurement from the ith observer to the target will be unavailable. The minimum of $D_\alpha(i)$ is achieved at $\alpha = \alpha^*$ given by

$$\alpha^* = -\frac{x_i(x - x_i) + y_i(y - y_i) + z_i(z - z_i)}{(x - x_i)^2 + (y - y_i)^2 + (z - z_i)^2} \tag{12.11}$$

Thus, we first examine whether $\alpha^* \in [0, 1]$ and then check the Earth blockage condition $D_{\alpha^*}(i) < R_E$.

12.3.2 Game Theoretic Formulation for Target Maneuvering Onset Time

We consider the case that a single observer tracks a single space target. Initially, the observer knows the target's state and the target also knows the observer's state. Assume that the target can only apply a T second burn that produces a specific thrust $\mathbf{w}$ with a maximum acceleration of a m/s^2. The goal of the target is to determine the maneuvering onset time and the direction of the thrust so that the resulting orbit will have the maximum duration of the Earth blockage to the observer. The goal of the observer is to maintain the target track with the highest estimation accuracy. To achieve this, the observer has to determine the sensor revisit time and cuing region as well as notify other observers having better geometry when Earth blockage occurs. Without loss of generality, we assume that the target can transfer its orbit to the same plane as the observer. In this case, when the target is at the opposite side of the Earth with respect to the observer and rotating in the same direction as the observer, the duration of the Earth blockage will be the maximum compared with other orbits with the same orbital elements except the inclinations. Note that in the pursuit–evasion game confined to a two dimensional plane, the minimax solution requires that the target applies the same thrust angle as the observer's (see Appendix 4 for details). Thus, an intelligent target will choose its maneuvering onset time as soon as its predicted observer's orbital trajectory has the Earth blockage. The corresponding maneuvering thrust will follow the minimax solution to the pursuit–evasion game.

When a target is tracked by multiple space borne observers, an observer can predict the target's maneuvering motion based on its estimated target state and the corresponding response of the pursuit–evasion game from the target where the terminal condition will lead to the Earth blockage to the observer. Thus, there is a need for the sensor manager to select the appropriate set of sensors that can persistently monitor all the targets especially when they maneuver.

12.3.3 Nonlinear Filter Design for Space Target Tracking

When a space target has been detected, the filter will predict the target state at any time instance in the future based on the available sensor measurements. Denote by $\hat{\mathbf{x}}_k^-$ the state prediction from time t_{k-1} to time t_k based on the state estimate $\hat{\mathbf{x}}_{k-1}^+$ at time t_{k-1} with all measurements up to t_{k-1}. The prediction is made by numerically integrating the state equation given by

$$\dot{\hat{\mathbf{x}}}(t) = f\big(\hat{\mathbf{x}}(t)\big) \tag{12.12}$$

without process noise. The mean square error (MSE) of the state prediction is obtained by numerically integrating the following matrix equation

$$\dot{P}(t) = F\big(\hat{\mathbf{x}}_k^-\big)P(t) + P(t)F\big(\hat{\mathbf{x}}_k^-\big)^T + Q(t) \tag{12.13}$$

where $F(\hat{\mathbf{x}}_k^-)$ is the Jacobian matrix given by

$$F(\mathbf{x}) = \begin{bmatrix} 0_{3\times 3} & I_3 \\ F_0(\mathbf{x}) & 0_{3\times 3} \end{bmatrix} \tag{12.14}$$

$$F_0(\mathbf{x}) = \mu \begin{bmatrix} \frac{3x^2}{r^5} - \frac{1}{r^3} & \frac{3xy}{r^5} & \frac{3xz}{r^5} \\ \frac{3xy}{r^5} & \frac{3y^2}{r^5} - \frac{1}{r^3} & \frac{3yz}{r^5} \\ \frac{3xz}{r^5} & \frac{3yz}{r^5} & \frac{3z^2}{r^5} - \frac{1}{r^3} \end{bmatrix} \tag{12.15}$$

$$r = \sqrt{x^2 + y^2 + z^2} \tag{12.16}$$

and evaluated at $\mathbf{x} = \hat{\mathbf{x}}_k^-$. The measurement $\mathbf{z}_k$ obtained at time t_k is given by

$$\mathbf{z}_k = h(\mathbf{x}_k) + \mathbf{v}_k \tag{12.17}$$

where

$$\mathbf{v}_k \sim \mathcal{N}(0, R_k) \tag{12.18}$$

is the measurement noise, which is assumed independent of each other and independent to the initial state as well as process noise.

The recursive linear minimum mean square error (LMMSE) filter applies the following update equation [2]

$$\hat{\mathbf{x}}_{k|k} \triangleq E^*\left[\mathbf{x}_k | \mathbf{Z}^k\right] = \hat{\mathbf{x}}_{k|k-1} + K_k \tilde{\mathbf{z}}_{k|k-1} \tag{12.19}$$

$$P_{k|k} = P_{k|k-1} - K_k S_k K_k' \tag{12.20}$$

where

$$\begin{aligned} \hat{\mathbf{x}}_{k|k-1} &= E^*\left[\mathbf{x}_k | \mathbf{Z}^{k-1}\right] \\ \hat{\mathbf{z}}_{k|k-1} &= E^*\left[\mathbf{z}_k | \mathbf{Z}^{k-1}\right] \\ \tilde{\mathbf{x}}_{k|k-1} &= \mathbf{x}_k - \hat{\mathbf{x}}_{k|k-1} \\ \tilde{\mathbf{z}}_{k|k-1} &= \mathbf{z}_k - \hat{\mathbf{z}}_{k|k-1} \\ P_{k|k-1} &= E\left[\tilde{\mathbf{x}}_{k|k-1} \tilde{\mathbf{x}}_{k|k-1}'\right] \\ S_k &= E\left[\tilde{\mathbf{z}}_{k|k-1} \tilde{\mathbf{z}}_{k|k-1}'\right] \\ K_k &= C_{\tilde{\mathbf{x}}_k \tilde{\mathbf{z}}_k} S_k^{-1} \\ C_{\tilde{\mathbf{x}}_k \tilde{\mathbf{z}}_k} &= E\left[\tilde{\mathbf{x}}_{k|k-1} \tilde{\mathbf{z}}_{k|k-1}'\right] \end{aligned}$$

Note that $E^*[\cdot]$ becomes the conditional mean of the state for linear Gaussian dynamics and the above filtering equations become the celebrated Kalman filter [2]. For nonlinear dynamic system, (12.19) is optimal in the mean square error sense when the state estimate is constrained to be an affine function of the measurement.

Given the state estimate $\hat{\mathbf{x}}_{k-1|k-1}$ and its error covariance $P_{k-1|k-1}$ at time t_{k-1}, if the state prediction $\hat{\mathbf{x}}_{k|k-1}$, the corresponding error covariance $P_{k|k-1}$, the measurement prediction $\hat{\mathbf{z}}_{k|k-1}$, the corresponding error covariance S_k, and the crosscovariance $E[\tilde{\mathbf{x}}_{k|k-1}\tilde{\mathbf{z}}'_{k|k-1}]$ in (12.19) and (12.20) can be expressed as a function only through $\hat{\mathbf{x}}_{k-1|k-1}$ and $P_{k-1|k-1}$, then the above formula is truly recursive. However, for general nonlinear system dynamics (12.3) and measurement equation (12.17) , we have

$$\hat{\mathbf{x}}_{k|k-1} = E^*\left[\int_{t_{k-1}}^{t_k} f\big(\mathbf{x}(t), \mathbf{w}(t)\big)\, dt + \mathbf{x}_{k-1} | \mathbf{Z}^{k-1}\right] \tag{12.21}$$

$$\hat{\mathbf{z}}_{k|k-1} = E^*\big[h(\mathbf{x}_k, \mathbf{v}_k) | \mathbf{Z}^{k-1}\big] \tag{12.22}$$

Both $\hat{\mathbf{x}}_{k|k-1}$ and $\hat{\mathbf{z}}_{k|k-1}$ will depend on the measurement history $\mathbf{Z}^{k-1}$ and the corresponding moments in the LMMSE formula. In order to have a truly recursive filter, the required terms at time t_k can be obtained *approximately* through $\hat{\mathbf{x}}_{k-1|k-1}$ and $P_{k-1|k-1}$, i.e.,

$$\{\hat{\mathbf{x}}_{k|k-1}, P_{k|k-1}\} \approx \text{Pred}\big[f(\cdot), \hat{\mathbf{x}}_{k-1|k-1}, P_{k-1|k-1}\big]$$
$$\{\hat{\mathbf{z}}_{k|k-1}, S_k, C_{\tilde{\mathbf{x}}_k \tilde{\mathbf{z}}_k}\} \approx \text{Pred}\big[h(\cdot), \hat{\mathbf{x}}_{k|k-1}, P_{k|k-1}\big]$$

where $\text{Pred}[f(\cdot), \hat{\mathbf{x}}_{k-1|k-1}, P_{k-1|k-1}]$ denotes that $\{\hat{\mathbf{x}}_{k-1|k-1}, P_{k-1|k-1}\}$ propagates through the nonlinear function $f(\cdot)$ to approximate $E^*[f(\cdot)|\mathbf{Z}^{k-1}]$ and the corresponding error covariance $P_{k|k-1}$.

Similarly, $\text{Pred}[h(\cdot), \hat{\mathbf{x}}_{k|k-1}, P_{k|k-1}]$ predicts the measurement and the corresponding error covariance only through the approximated state prediction. This poses difficulties for the implementation of the recursive LMMSE filter due to insufficient information. The prediction of a random variable going through a nonlinear function, most often, can not be completely determined using only the first and second moments. Two remedies are often used: One is to approximate the system to the best extent such that the prediction based on the approximated system can be carried out only through $\{\hat{\mathbf{x}}_{k-1|k-1}, P_{k-1|k-1}\}$ [20]. Another is by approximating the density function with a set of particles and propagating those particles in the recursive Bayesian filtering framework, i.e., using a particle filter [8].

12.3.4 Posterior Cramer–Rao Lower Bound of the State Estimation Error

Denote by $J(t)$ the Fisher information matrix. Then the posterior Cramer–Rao lower bound (PCRLB) is given by [18]

$$B(t) = J(t)^{-1} \tag{12.23}$$

which quantifies the ideal mean square error of any filtering algorithm, i.e.,

$$E\left[\left(\hat{\mathbf{x}}(t_k)-\mathbf{x}(t_k)\right)\left(\hat{\mathbf{x}}(t_k)-\mathbf{x}(t_k)\right)^T|\mathbf{Z}^k\right]\geq B(t_k) \tag{12.24}$$

Assuming an additive white Gaussian process noise model, the Fisher information matrix satisfies the following differential equation

$$\dot{J}(t)=-J(t)F(\mathbf{x})-F(\mathbf{x})^T J(t)-J(t)Q(t)J(t) \tag{12.25}$$

for $t_{k-1}\leq t\leq t_k$ where F is the Jacobian matrix given by

$$F(\mathbf{x})=\frac{\partial f(\mathbf{x})}{\partial \mathbf{x}} \tag{12.26}$$

When a measurement is obtained at time t_k with additive Gaussian noise $\mathcal{N}(0, R_k)$, the new Fisher information matrix is

$$J(t_k^+)=J(t_k^-)+E_{\mathbf{x}}\left[H(\mathbf{x})^T R_k^{-1}H(\mathbf{x})\right] \tag{12.27}$$

where H is the Jacobian matrix given by

$$H(\mathbf{x})=\frac{\partial h(\mathbf{x})}{\partial \mathbf{x}} \tag{12.28}$$

See Appendix 3 for the numerical procedure to evaluate the Jacobian matrix for a non-perturbed orbital trajectory propagation. The initial condition for the recursion is $J(t_0)$ and the PCRLB can be obtained with respect to the true distribution of the state $\mathbf{x}(t)$. In practice, the sensor manager will use the estimated target state to compute the PCRLB for any time instance of interest and decide whether a new measurement has to be made to improve the estimation accuracy.

12.4 Sensor Management for Situation Awareness

12.4.1 Information Theoretic Measure for Sensor Assignment

In sensor management, each observer has to decide when to measure which target so that the performance gain in terms of a certain metric can be maximized. For a Kalman filter or its extension for the nonlinear dynamic state or measurement equations, namely, the recursive LMMSE filter, the error covariance of the state estimate has the following recursive form [2].

$$P_{k+1|k+1}^{-1}=P_{k+1|k}^{-1}+H(\mathbf{x}_{k+1})^T R_{k+1}^{-1}H(\mathbf{x}_{k+1}) \tag{12.29}$$

Thus the information gain from the sensor measurement at time t_{k+1} in terms of the inverse of the state estimation error covariance is $H(\mathbf{x}_{k+1})^T R_{k+1}^{-1}H(\mathbf{x}_{k+1})$ where R_{k+1} is the measurement error covariance. Consider M observers each of which can

measure at most one target at any sampling time. When there are N space targets being tracked by M observers, sensor assignment is concerned with the sensor to target correspondence so that the total information gain can be maximized. Denote by χ_{ij} the assignment of observer i to target j at any particular time t_{k+1}. The sensor assignment problem is

$$\min_{\chi_{ij}} c_{ij}\chi_{ij} \tag{12.30}$$

$$\text{subject to} \quad \sum_{i=1}^{M} \chi_{ij} \leq 1, \quad j = 1, \ldots, N; \tag{12.31}$$

$$\sum_{j=1}^{N} \chi_{ij} \leq 1, \quad i = 1, \ldots, M; \tag{12.32}$$

and $\chi_{ij} \in \{0, 1\}$. The cost c_{ij} is

$$c_{ij} = \mathrm{Tr}\big\{H\big(\mathbf{x}_j\big((t_{k+1})\big)\big)^T R_i^{-1}(t_{k+1}) H_i\big(\mathbf{x}_j\big((t_{k+1})\big)\big)\big\} \tag{12.33}$$

if there is no Earth blockage between observer i to target j. In the above formulation, all targets are assumed to have the same importance so the observes are scheduled to make the most informative measurements. This may lead to a greedy solution where those targets close to the observers will be tracked more accurately than those away from the observers. It may not achieve the desired tracking accuracy for each target.

12.4.2 Covariance Control for Sensor Scheduling

Covariance control method does not optimize a performance metric directly in the sensor-to-target assignment, instead, it requires the filter designer to specify a desired state estimation error covariance so that the selection of sensors and the corresponding sensing times will meet the specified requirements after the tracker update using the sensor measurements as scheduled. Denote by $P_d(t_{k+1})$ the desired error covariance of the state estimation at time t_{k+1}. Then the need of a sensor measurement at t_{k+1} for this target, according to the covariance control method, is

$$n(t_{k+1}) = -\min\big(\mathrm{eig}\big\{P_d(t_{k+1}) - P_{k+1|k}\big\}\big) \tag{12.34}$$

where the negative sign has the following implication: A positive value of the eigenvalue difference implies that the desired covariance requirement is not met. The goal of covariance control is to minimize the total sensing cost so that all the desired covariance requirements are met. If we use the same notation c_{ij} as the cost for the observer i to sense the target j at t_{k+1}, then the covariance control tries to solve the

following optimization problem.

$$\min_{\chi_{ij}} c_{ij}\chi_{ij} \tag{12.35}$$

$$\text{subject to} \quad n_{ij}(t_{k+1}) = -\min\left(\text{eig}\left\{P_{dij}(t_{k+1}) - P_{k+1|k+1}(\chi_{ij})\right\}\right) \leq 0,$$
$$i = 1, \ldots, M, \;\; j = 1, \ldots, N \tag{12.36}$$

and $\chi_{ij} \in \{0, 1\}$. In this setting, more than one observer can sense the same target at the same time. The optimization problem is combinatorial in nature and one has to evaluate 2^{MN} possible sensor-to-target combinations in general, which is computationally prohibitive. Alternatively, a suboptimal need-based greedy algorithm has been proposed [10]. It also considers the case where certain constraints can not be met, i.e., the desired covariance is unachievable even with all the sensing resources.

12.4.3 Game Theoretic Covariance Prediction for Sensor Management

In the formulation of the sensor management problem, we need the filter to provide the information on the state estimation error covariance which is based on the orbital trajectory propagation assuming that the target does not maneuver. If the target maneuvers, then the filter calculated error covariance assuming the non-maneuver motion model will be too optimistic. There are two possible approaches to account for the target maneuver motion. One is to detect target maneuver and estimate its onset time as quickly as possible [15]. Then the filter will be adjusted with larger process noise covariance to account for the target maneuvering motion. Alternatively, one can design a few typical target maneuvering motion models and run a multiple model estimator with both non-maneuver and maneuver motion models [2]. The multiple model filter will provide the model conditioned state estimation error covariances as well as the unconditional error covariance for sensor management purposes. Note that the multiple model estimator does not make a hard decision on which target motion model is in effect at any particular time, but evaluates the probability of each model. The corresponding unconditional covariance immediately after target maneuver onset time can still be very optimistic, which is needed to support the evidence that a maneuvering motion model is more likely than a non-maneuvering one. As a consequence, the scheduled sensing action in response to the target maneuver based on the unconditional covariance from a multiple model estimator can be too late for evasive target motion.

We propose to use generalized Page's test for detecting target maneuver [15] and apply the *model conditioned* error covariance from each filter in the sensor management. Denoted by $S_m(t_{k+1})$ the set of targets being classified as in the maneuvering mode and $S_{-m}(t_{k+1})$ the set of targets in the nonmaneuvering model, respectively. We apply covariance control for sensor-to-target allocation only to those targets in $S_m(t_{k+1})$ and use the remaining sensing resources to those targets in $S_{-m}(t_{k+1})$ by maximizing the information gain. The optimization problem becomes

$$\min_{\chi_{ij}} c_{ij}\chi_{ij} \tag{12.37}$$

$$\text{subject to} \quad n_{ij}(t_{k+1}) = -\min\left(\text{eig}\left\{P_{dij}(t_{k+1}) - P_{k+1|k+1}(\chi_{ij})\right\}\right) \le 0,$$
$$i = 1, \ldots, M, \ j \in S_m(t_{k+1}) \tag{12.38}$$

$$\sum_{i=1}^{M} \chi_{ij} \le 1, \quad j \in S_{-m}(t_{k+1}) \tag{12.39}$$

$$\sum_{j \in S_{-m}(t_{k+1})} \chi_{ij} \le 1, \quad i = 1, \ldots, M \tag{12.40}$$

and $\chi_{ij} \in \{0, 1\}$. The cost c_{ij} is

$$c_{ij} = \begin{cases} \text{Tr}\left\{H\left(\mathbf{x}_j\left((t_{k+1})\right)\right)^T R_i^{-1}(t_{k+1}) H_i\left(\mathbf{x}_j\left((t_{k+1})\right)\right)\right\} & j \in S_{-m}(t_{k+1}) \\ 0 & j \in S_m(t_{k+1}) \end{cases} \tag{12.41}$$

Given that target $j \in S_{-m}(t_k)$, we assume that observer i will declare $j \in S_m(t_{k+1})$ if the predicted target location has Earth blockage to the observer i at t_{k+1}. If the target is declared as in the maneuvering mode, then the predicted error covariance will be based on the worst case scenario of the pursuit–evasion game between the observer and the target (see Appendix 4 for details).

12.5 Simulation Study

12.5.1 Scenario Description

We consider a small scale space target tracking scenario where four satellite observers collaboratively track two satellite targets. The nominal orbital trajectories are generated from realistic satellite targets selected in the SpaceTrack database. The four observer satellites are (1) ARIANE 44L, (2) OPS 856, (3) VANGUARD 1, and (4) ECHO 1. They are in low-Earth orbits. The two target satellites are: (1) ECHOSTAR 10, and (2) COSMOS 2350. They are in geostationary orbits. The simulation was based on the software package that utilizes the general mission analysis tool (GMAT).[1] Figure 12.1 shows the orbital trajectories of the observers and targets. The associated tracking errors were obtained based on the recursive linear minimum mean square error filter when sensors are assigned to targets according to the nonmaneuvering motion. The error increases in some time segments are due to the Earth blockage where no measurements are available from any observer.

[1]General Mission Analysis Tool, released by National Aeronautics and Space Administration (NASA), available at http://gmat.gsfc.nasa.gov/.

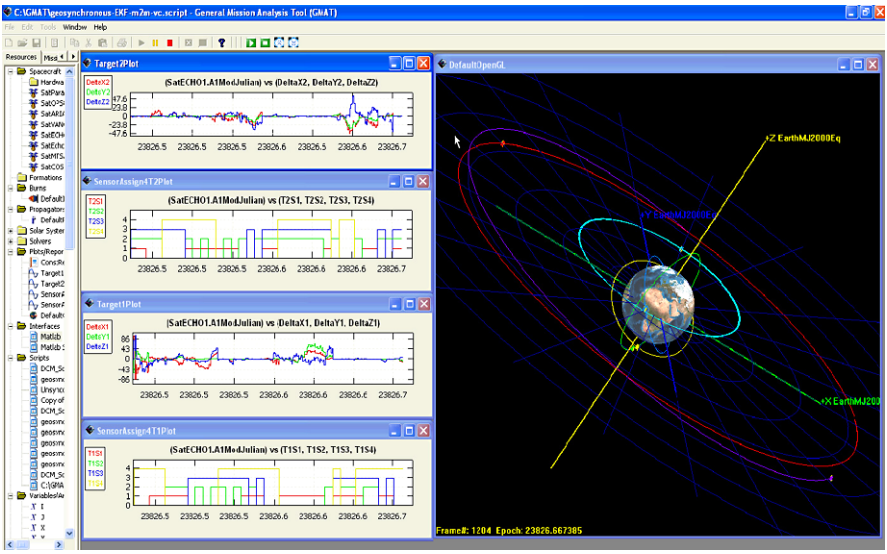

Fig. 12.1 The space target tracking scenario where four observers collaboratively track two targets

12.5.2 Performance Comparison

We now consider the case in which the target performs an unknown thrust maneuver that changes the eccentricity of its orbit. In particular, both targets are initially in the GEO orbit and at time $t = 1000$ s, target 1 performs a 1 s burn that produces a specific thrust, i.e., an acceleration $w = [0\ 0.3\ 0]^T$ km/s^2, while, at time $t = 1500$ s, target 2 performs a 1 s burn that produces a specific thrust $w = [0\ 0.5\ 0]^T$ km/s^2. The eccentricity change of target 1 after the burn is around $e \approx 0.35$ while the eccentricity change of target 2 after the second burn is $e \approx 0.59$. Another type of target maneuver is the inclination change produced by a specific thrust. Two inclination changes are generated with $i \approx 0.16$ for target 1 and $i \approx 0.09$ for target 2. Each observer has the minimal sampling interval of 50 s and we assume that all observers are synchronized and the sensor manager can make centralized coordination based on the centralized estimator for each target. We consider two cases: (i) the observer has range and angle measurements with standard deviations 0.1 km and 10 mrad, respectively, and (ii) the observer has range, angle and range rate measurements with standard deviations 0.1 km, 10 mrad, 2 m/s, respectively.

We applied the generalized Page's test (GPT) without and with range rate measurement for maneuver detection while the filter update of state estimate does not use the range rate measurement [15]. The reason is that the nonlinear filter designed assuming non-maneuver target motion is sensitive to the model mismatch in the range rate when target maneuvers. The thresholds of the generalized Page's test for both case (i) and case (ii) were chosen to have the false alarm probability $P_{FA} = 1\%$. The average delays of target maneuver onset detection for both cases are measured in terms of the average number of observations from the maneuver onset time to

Table 12.1 Comparison of tracking accuracy for various orbital changes of the targets

Cases	$e \to 0.35$	$e \to 0.59$	$i \to 0.09$	$i \to 0.16$
(i) Average delay per observations	7.3	6.4	12.1	9.6
(i) PTR, peak position error (km)	33.7	54.8	14.5	18.9
(i) IMM, peak position error (km)	48.1	66.5	12.4	22.3
(i) PTR, peak velocity error (km/s)	0.38	0.40	0.22	0.25
(i) IMM, peak velocity error (km/s)	0.41	0.44	0.21	0.26
(ii) Average delay per observations	1.3	1.0	2.9	2.4
(ii) PTR, peak position error (km)	6.9	7.4	3.1	3.8
(ii) IMM, peak position error (km)	8.3	11.2	3.2	4.1
(ii) PTR, peak velocity error (km/s)	0.28	0.31	0.16	0.19
(ii) IMM, peak velocity error (km/s)	0.30	0.34	0.16	0.21

the declaration of the target maneuver. Once target maneuver is declared, then another filter assuming the white noise acceleration with process noise spectrum of 0.6 km/s^2 was used along both tangential and normal directions of the estimated target motion. Alternatively, an interacting multiple model (IMM) estimator [2] with nonmaneuver and maneuver motion models using the same parameter settings as the model switching filters embedded in the target maneuvering detector was used to compare the tracking accuracy. Table 12.1 compares the peak errors in position and velocity for each target maneuvering motion using model switching filter and the IMM estimator. The average detection delays for both cases are also shown in Table 12.1 for GPT algorithm. We can see that the range rate measurement, if available, can improve the average detection delay of target maneuver significantly and thus reducing the peak estimation errors in both target position and velocity. The model switching filter using GPT has better tracking accuracy than the IMM estimator in most cases even for the peak errors. It should be clear that the filter based on nonmaneuver motion model outperforms the IMM estimator during the segment that the target does not have an orbital change. Interestingly, even though the inclination change takes longer time to detect compared with the eccentricity change for both targets, the resulting peak estimation errors in position and velocity are relatively smaller for both the model switching filter and the IMM estimator. The extensive comparison among other nonlinear filtering methods for space target tracking can be found in [4].

Next, we assume that both target 1 and target 2 will choose their maneuver onset times intelligently based on their geometries to the observers. Both targets can have a maximum acceleration of 0.05 km/s^2 with a maximum of 10 s burn. We assume that each observer can measure target range, angle, and range rate with the same accuracy as in the case (ii) of the tracking scenario considered previously. We implemented the following configurations of the sensor management schemes to determine which observer measures which target at a certain time instance. (i) Information based method: Sensors are allocated with a uniform sampling interval of 50 s to maximize the information gain. (ii) Covariance control based method: Sen-

Table 12.2 Performance comparison for various sensor management methods

Configuration	Peak position error (km)	Average position error (km)	Peak velocity error (km/s)	Average velocity error (km/s)	Average sampling interval (s)
(i) Target 1	89.7	24.4	2.1	0.16	50
(i) Target 2	76.3	14.2	1.6	0.14	50
(ii) Target 1	16.7	2.4	0.36	0.10	13.5
(ii) Target 2	15.2	1.8	0.29	0.09	16.8
(iii) Target 1	12.2	1.8	0.28	0.08	37.6
(iii) Target 2	10.9	1.3	0.27	0.08	39.2

sors are scheduled with the sampling interval such that the desired position error is within 10 km for each target. The state prediction error covariance for nonmaneuver or maneuver motion model is computed based on the posterior Cramer–Rao lower bound. (iii) Game theoretic method: Sensors are allocated by maximizing the information gain for nonmaneuvering targets and covariance control will be applied to maneuvering targets. The maneuvering onset time is predicted based on the pursuit evasion game for each observer-to-target pairing. In all three configurations, model switching filter is used for tracking each target. We compare the peak and average errors in position and velocity for both targets as well as the average sampling interval from all observers for configurations (i)–(iii). The results are listed in Table 12.2. We can see that the information based method (configuration (i)) yields the largest peak errors among the three schemes. This is due to the fact that both targets apply evasive maneuver so that the peak errors will be much larger compared with the results in Table 12.1 based on the same tracker design and sampling interval. In order to achieve the desired position error, covariance control method (configuration (ii)) achieves much smaller peak and average errors compared with configuration (i) at the price of making the sampling interval much shorter. Note that the peak position errors are larger than 10 km for both targets owing to the detection delay of maneuvering onset time. The proposed game theoretic method (configuration (iii)) has the smallest peak and average errors because of the prediction of maneuvering onset time by modeling target evasive motion from the pursuit evasion game. Note that it also has longer average sampling interval than that of configuration (ii) due to a quicker transient when each target stops its burn, indicating possible energy saving for the overall system. The sensing resources saved with configuration (iii) can also be applied to search other potential targets in some designated cells. One possible approach to perform joint search and tracking of space targets was discussed in [5].

12.6 Summary and Conclusions

In space target tracking by satellite observers, it is crucial to assign the appropriate sensor set to each target and minimizes the Earth blockage period. With complete

knowledge of the space borne observers, a target may engage its evasive maneuvering motion immediately after the Earth blockage occurs and change its orbit to maximize the duration of the Earth blockage. We presented a game theoretic model for the determination of maneuvering onset time and consequently, the covariance control is applied to the maneuvering targets in the sensor-to-target assignment. For nonmaneuvering targets, we try to maximize the total information gain by selecting sensors that will provide the most informative measurements on the target's state. We simulated a multi-observer multi-target tracking scenario where four LEO observers collaboratively track two GEO targets. We found that the multiple model estimator assuming random maneuvering onset time yields much larger estimation error compared with the model switching tracker based on maneuvering detection from the solution to the pursuit–evasion game. In addition, sensor assignment based on maximum information gain can lead to large tracking error for evasive targets while using the same desired error covariance for all targets can only alleviate the issue at the price of more frequent revisit time for each target. Fortunately, the sensor assignment based on covariance control for maneuvering targets and maximum information gain for nonmaneuvering targets achieves a reasonable tradeoff between the tracking accuracy and the consumption of sensing resources.

There are many avenues to extend the existing work in order to achieve space situational awareness. First, target intent can be inferred based on its orbital history. It is of great interest to separate the nonevasive and evasive orbital maneuvering motions and allocate the sensing resources accordingly. Second, our model of the pursuit–evasion game relies on the complete knowledge of the observer's and target's state which may not be known to both players in real life. This poses challenges in the development of the game theoretic model with incomplete information which is computationally tractable for the sensor management to allocate sensing resources ahead of time. Finally, the current nonlinear filter does not consider the clutter and closely spaced targets where imperfect data association has to be handled by the filtering algorithm. It should be noted that the posterior Cramer–Rao lower bound for single target tracking with random clutter and imperfect detection [19] can be readily applied to the covariance control. However, it is still an open research problem to design efficient nonlinear filtering method that can achieve the theoretical bound of the estimation error covariance.

Acknowledgement This work was supported in part by the US Air Force under contracts FA8650-09-M-1552 and FA9453-09-C-0175, US Army Research Office under contract W911NF-08-1-0409, Louisiana Board of Regents NSF(2009)-PFUND-162, and the Office of Research and Sponsored Programs, the University of New Orleans.

Appendix 1: Conversion of the Coordinate Systems

The following conversion schemes among different coordinate systems are based on [3]. Given the position $\mathbf{r} = [\xi \ \eta \ \zeta]'$ in the ECEF frame, the latitude φ, longitude λ and altitude h (which are the three components of $\mathbf{r}_{geo}$) are determined by

STEP 1 $\varphi = 0$

repeat

$\varphi_{\text{old}} = \varphi$

$D_\varphi = R_e\left[1 - \epsilon_e \sin^2 \varphi_{\text{old}}\right]^{-\frac{1}{2}}$

$\varphi = \text{atan}\left(\dfrac{\zeta + D_\varphi \epsilon_e^2 \sin \varphi_{\text{old}}}{\sqrt{\xi^2 + \eta^2}}\right)$

until $|\varphi - \varphi_{\text{old}}| < TOL$

STEP 2 $\lambda = \text{atan}(\frac{\eta}{\xi})$

$h = \dfrac{\zeta}{\sin \varphi} - D_\varphi\left(1 - \epsilon_e^2\right)$

where $R_e = 6378.137$ km and $\epsilon_e = 0.0818191$ are the equatorial radius and eccentricity of the Earth, respectively. *TOL* is the error tolerance (e.g., 10^{-10}) and the convergence occurs normally within 10 iterations.

The origin of the local Cartesian frame $\mathbf{O}$ is given by

$$\mathbf{O} = \begin{bmatrix} 0 & D_\varphi \epsilon_e^2 \sin \varphi \cos \varphi & D_\varphi\left(\epsilon_e^2 \sin^2 \varphi - 1\right) \end{bmatrix}' \tag{12.42}$$

and the rotation matrix is given by

$$A = \begin{bmatrix} -\sin \lambda & \cos \lambda & 0 \\ -\sin \varphi \cos \lambda & -\sin \varphi \sin \lambda & \cos \varphi \\ \cos \varphi \cos \lambda & \cos \varphi \sin \lambda & \sin \varphi \end{bmatrix} \tag{12.43}$$

The position $\mathbf{r}$ in the local Cartesian frame is given by

$$\mathbf{r}_{\text{loc}} = A\mathbf{r} + \mathbf{O} \tag{12.44}$$

Appendix 2: Keplerian Elements

The *specific angular momentum* lies normal to the orbital plane given by $\mathbf{h} = \mathbf{r} \times \mathbf{v}$ with magnitude $h \triangleq \|\mathbf{h}\|$. *Inclination* is the angle between the equatorial plane and the orbital plane given by $i \triangleq \cos^{-1}(\frac{h_z}{h})$ where h_z is the z-component of $\mathbf{h}$. *Eccentricity* of the orbit is given by

$$\mathbf{e} \triangleq \frac{1}{\mu}\left[\left(v^2 - \frac{\mu}{r}\right)\mathbf{r} - r v_r \mathbf{v}\right] \tag{12.45}$$

with magnitude $e \triangleq \|\mathbf{e}\|$. The longitude of the ascending node is given by

$$\Omega \triangleq \begin{cases} \cos^{-1}(\frac{n_x}{n}) & n_y \geq 0 \\ 2\pi - \cos^{-1}(\frac{n_x}{n}) & n_y < 0 \end{cases} \tag{12.46}$$

where $\mathbf{n}$ is the vector pointing towards the ascending node with magnitude $n \triangleq \|\mathbf{n}\|$. The *argument of perigee* is angle between the node line and the eccentricity vector given by

$$\omega \triangleq \begin{cases} \cos^{-1}(\frac{\mathbf{ne}}{ne}) & e_z > 0 \\ 2\pi - \cos^{-1}(\frac{\mathbf{ne}}{ne}) & e_z < 0 \end{cases} \tag{12.47}$$

with the convention that

$$\omega = \cos^{-1}\left(\frac{e_x}{e}\right) \tag{12.48}$$

for an equatorial orbit. The *true anomaly* ν is the angle between the eccentricity vector and the target's position vector given by

$$\nu \triangleq \begin{cases} \cos^{-1}(\frac{\mathbf{er}}{er}) & v_r > 0 \\ 2\pi - \cos^{-1}(\frac{\mathbf{er}}{er}) & v_r < 0 \end{cases} \tag{12.49}$$

with the convention that $\nu = \cos^{-1}(\frac{r_x}{r})$ for a circular orbit. The *eccentric anomaly* is the angle between apogee and the current position of the target given by

$$E = \cos^{-1}\left(\frac{1 - r/a}{e}\right) \tag{12.50}$$

where a is the orbit's semi-major axis given by $a = \frac{1}{\frac{2}{r} - \frac{v^2}{\mu}}$. The *mean anomaly* is $M = E - e \sin E$. The orbital period is given by $T = 2\pi\sqrt{\frac{a^3}{\mu}}$.

The six Keplerian elements are $\{a, i, \Omega, \omega, e, M\}$. The orbit of a space target can be fully determined by the parameter set $\{i, \Omega, \omega, T, e, M\}$ with initial condition given by the target position at any particular time [17]. The angles $\{i, \Omega, \omega\}$ transform the inertial frame to the orbital frame while T and e specify the size and shape of the ellipsoidal orbit. The time dependent parameter $\nu(t)$ represents the position of the target along its orbit in the polar coordinate system.

Appendix 3: Algorithm for Orbital State Propagation

Presented below is an algorithm that propagates the state of an object in an orbital trajectory around the Earth following [3]. Both the trajectory propagation and the corresponding Jacobian matrix of the nonlinear orbital equation are given. Let $x(t)' = [\mathbf{r}(t)' \ \dot{\mathbf{r}}(t)']$ be the unknown state to be computed at time t, given the state $x_0' = \mathbf{x}(t_0)' = [\mathbf{r}_0' \dot{\mathbf{r}}_0']$ at the time t_0. The gravitational parameter $\mu = 3.986012 \times 10^5$ km^3/sec^2 and the convergence check parameter $TOL = 10^{-10}$ are used.

STEP 1 $r_0 := \|\mathbf{r}_0\|; \quad v_0 := \|\dot{\mathbf{r}}_0\|; \quad q_0 := \frac{1}{\mu}\mathbf{r}_0'\dot{\mathbf{r}}_0$

$$a_0 := \frac{2}{r_0} - \frac{v_0^2}{\mu}; \quad p_0 := \frac{1 - a_0 r_0}{\sqrt{\mu}}$$

STEP 2 $\alpha := \frac{a_0(t - t_0)}{\sqrt{\mu}}; \quad \beta := a_0\alpha^2$

STEP 3 $c := \frac{1 - \cos(\sqrt{\beta})}{\beta}; \quad s := \frac{\sqrt{\beta} - \sin(\sqrt{\beta})}{\beta\sqrt{\beta}}$

STEP 4 $\tau := p_0\alpha^3 s + q_0\alpha^2 c + \frac{r_0}{\sqrt{\mu}}\alpha$

$$\frac{\mathrm{d}\tau}{\mathrm{d}\alpha} := p_0\alpha^2 c + q_0\alpha(1 - s\beta) + \frac{r_0}{\sqrt{\mu}}$$

$$\alpha := \alpha + \left[\frac{\mathrm{d}\tau}{\mathrm{d}\alpha}\right]^{-1}\left[(t - t_0) - \tau\right]$$

STEP 5 if$\left(\left[(t - t_0) - \tau\right] > TOL\right)$

gotoSTEP 3

STEP 6 $f := 1 - \frac{\alpha^2 c}{r_0}; \quad g := (t - t_0) - \frac{\alpha^3 s}{\sqrt{\mu}}$

$$\mathbf{r}(t) := f\mathbf{r}_0 + g\dot{\mathbf{r}}_0; \quad r := \left\|\mathbf{r}(t)\right\|$$

STEP 7 $\dot{f} := \left(\frac{\sqrt{\mu}}{r_0}\right)(s\beta - 1)\left(\frac{\alpha}{r}\right); \quad \dot{g} := 1 - \frac{\alpha^2 c}{r}; \quad \dot{\mathbf{r}}(t) := \dot{f}\mathbf{r}_0 + \dot{g}\dot{\mathbf{r}}_0$

The above steps yield the required state $x(t)' = [\mathbf{r}(t)'\dot{\mathbf{r}}(t)']$ at time t. In order to predict the covariance of the position $\mathbf{r}(t)$ by propagating the covariance of $\mathbf{r}(t_0)$ from t_0 to t, we need to compute the 6×3 matrix $\nabla_{x_0}\mathbf{r}(t)$. The computation of this matrix involves the following additional steps.

STEP 8 $\nabla_{x_0} r_0 := \begin{bmatrix}\mathbf{r}_0 \\ 0\end{bmatrix}\left(\frac{1}{r_0}\right); \quad \nabla_{x_0} v_0 := \begin{bmatrix}0 \\ \dot{\mathbf{r}}_0\end{bmatrix}\left(\frac{1}{v_0}\right)$

$$\nabla_{x_0} q_0 := \begin{bmatrix}\dot{\mathbf{r}}_0 \\ \mathbf{r}_0\end{bmatrix}\left(\frac{1}{\mu}\right)$$

$$\nabla_{x_0} a_0 := (\nabla_{x_0} r_0)\left(\frac{-2}{r_0^2}\right) + (\nabla_{x_0} v_0)\left(\frac{-2v_0}{\mu}\right)$$

$$\nabla_{x_0} p_0 := (\nabla_{x_0} r_0)\left(\frac{-a_0}{\sqrt{\mu}}\right) + (\nabla_{x_0} a_0)\left(\frac{-r_0}{\sqrt{\mu}}\right)$$

$$\texttt{STEP 9} \quad \frac{\mathrm{d}s}{\mathrm{d}\beta} := \frac{c-3s}{2\beta}; \quad \frac{\mathrm{d}c}{\mathrm{d}\beta} := \frac{1-s\beta-2c}{2\beta}$$

$$\texttt{STEP 10} \quad b_1 := (\nabla_{x_0} q_0)\left(-\alpha^2 c\right) + (\nabla_{x_0} p_0)\left(-\alpha^3 s\right) + (\nabla_{x_0} r_0)\left(\frac{-\alpha}{\sqrt{\mu}}\right)$$

$$b_2 := (\nabla_{x_0} a_0)\left(-\alpha^2\right)$$

$$A := \begin{bmatrix} 3p_0\alpha^2 s + 2q_0\alpha c + \frac{r_0}{\sqrt{\mu}} & p_0\alpha^3 \frac{\mathrm{d}s}{\mathrm{d}\beta} + q_0\alpha^2 \frac{\mathrm{d}c}{\mathrm{d}\beta} \\ 2a_0\alpha & -1 \end{bmatrix}$$

$$\left[(\nabla_{x_0}\alpha)(\nabla_{x_0}\beta)\right] := [b_1 b_2] A^{-1}$$

$$\texttt{STEP 11} \quad \nabla_{x_0} f := \left[(\nabla_{x_0} r_0)\left(\frac{\alpha c}{r_0}\right) - (\nabla_{x_0}\alpha)(2c) - (\nabla_{x_0}\beta)\left(\alpha\frac{\mathrm{d}c}{\mathrm{d}\beta}\right)\right]\left[\frac{\alpha}{r_0}\right]$$

$$\nabla_{x_0} g := \left[(\nabla_{x_0}\alpha)(3s) - (\nabla_{x_0}\beta)\left(\alpha\frac{\mathrm{d}s}{\mathrm{d}\beta}\right)\right]\left[\frac{-\alpha^2}{\sqrt{\mu}}\right]$$

$$\texttt{STEP 12} \quad \nabla_{x_0}\mathbf{r}(t) = \begin{bmatrix} fI_3 \\ gI_3 \end{bmatrix} + (\nabla_{x_0} f)\mathbf{r}_0' + (\nabla_{x_0} g)\dot{\mathbf{r}}_0'.$$

Appendix 4: Pursuit Evasion Game in a 2D Plane

Consider the space target orbiting the Earth with the polar coordinate system fixed on the Earth's center. The motion of the target is given by

$$\ddot{r} - r\dot{\theta}^2 = -\frac{\mu}{r^2} + \frac{F\sin\alpha}{m} \tag{12.51}$$

$$r\ddot{\theta} + 2\dot{r}\dot{\theta} = \frac{F\cos\alpha}{m} \tag{12.52}$$

where α is the angle the thrust vector and the local horizontal as shown in Fig. 12.2. Denote by v_θ and v_r the tangential and radial velocities of the target, respectively. The dynamic equation of the space target can be written as

$$\dot{v}_r - \frac{v_\theta^2}{r} = -\frac{\mu}{r^2} + \frac{F\sin\alpha}{m} \tag{12.53}$$

$$\dot{v}_\theta + \frac{v_r v_\theta}{r} = \frac{F\cos\alpha}{m} \tag{12.54}$$

It is desirable to normalize the parameters with respect to a reference circular orbit with radius r_0 and velocity v_0, so that significant figures will not be lost due to linearizing the target motion equation. Define the following normalized state variables.

$$x_1 = \frac{r}{r_0} \tag{12.55}$$

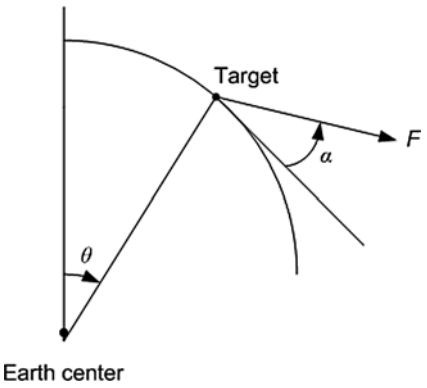

Fig. 12.2 Simplified 2D geometry of a space target

$$x_2 = \frac{v_r}{v_0} \tag{12.56}$$

$$x_3 = \frac{v_\theta}{v_0} \tag{12.57}$$

$$x_4 = \theta \tag{12.58}$$

Let $\tau = \frac{v_0}{r_0} t$. The state equation with respect to τ can be written as

$$\dot{x}_1 = x_2 \tag{12.59}$$

$$\dot{x}_2 = \frac{x_3^2}{x_1} - \frac{1}{x_1^2} + F_0 \sin\alpha \tag{12.60}$$

where $F_0 = \frac{r_0 F}{v_0^2 m}$ is a constant depending the thrust F and target's mass m.

$$\dot{x}_3 = -\frac{x_2 x_3}{x_1} + F_0 \cos\alpha \tag{12.61}$$

$$\dot{x}_4 = \frac{x_3}{x_1} \tag{12.62}$$

In the standard pursuit evasion game, the objective is to find the minimax solution, if exists, to the objective function

$$J = \phi\big(\mathbf{x}(t_f)\big) \tag{12.63}$$

with the state dynamics given by

$$\dot{\mathbf{x}} = f(\mathbf{x}, u, v, t) \tag{12.64}$$

and the initial condition $\mathbf{x}(t_0) = \mathbf{x}_0$ as well as the terminal constraint $\psi(\mathbf{x}(t_f)) = 0$. Here u and v represent the controls associated with the pursuer and the evader, respectively. The goal is to determine $\{u^*, v^*\}$ such that

$$J\big(u^*, v\big) \le J\big(u^*, v^*\big) \le J\big(u, v^*\big) \tag{12.65}$$

The necessary condition for the minimax solution to exist is that the costate $\boldsymbol{\lambda}$ satisfies the following transversality condition.

$$\boldsymbol{\lambda} = \phi_{\mathbf{x}}(t_f) + \nu\psi_{\mathbf{x}}(t_f) \tag{12.66}$$

$$H(t_f) = \phi_t(t_f) + \nu\psi_t(t_f) \tag{12.67}$$

where ν is a Lagrange multiplier and H is the Hamiltonian associated with $\boldsymbol{\lambda}$ that has to be optimized

$$H^* = \max_{v} \min_{u} H(\mathbf{x}, \boldsymbol{\lambda}, u, v, t) \tag{12.68}$$

It has been shown in [9] that at the optimal solution, the thrust angles of the pursuer and the evader are the same.

References

1. Bar-Shalom, Y., Blair, W.D.: Multitarget-Multisensor Tracking: Applications and Advances, vol. III. Artech House, Norwood (2000)
2. Bar-Shalom, Y., Li, X.R., Kirubarajan, T.: Estimation with Applications to Tracking and Navigation: Algorithms and Software for Information Extraction. Wiley, New York (2001)
3. Bate, R., et al.: Fundamentals of Astrodynamics. Dover, New York (1971)
4. Chen, H., Chen, G., Blasch, E., Pham, K.: Comparison of several space target tracking filters. In: Proc. SPIE Defense, Security Sensing, vol. 7730, Orlando, FL, USA (2009)
5. Chen, G., Chen, H., Pham, K., Blasch, E., Cruz, J.B.: Awareness-based game theoretic space resource management. In: Proc. SPIE Defense, Security Sensing, vol. 7730, Orlando, FL, USA (2009)
6. Duong, N., Winn, C.B.: Orbit determination by range-only data. J. Spacecr. Rockets **10**, 132–136 (1973)
7. Fowler, J.L., Lee, J.S.: Extended Kalman filter in a dynamic spherical coordinate system for space based satellite tracking. In: Proc. AIAA 23rd Aerospace Sciences Meeting. AIAA-85-0289, Reno, NV (1985)
8. Gordon, N., Salmond, D., Smith, A.: Novel approach to nonlinear/non-Gaussian Bayesian state estimation. IEE Proc. F **140**, 107–113 (1993)
9. Isaacs, R.: A Mathematical Theory with Applications to Warfare and Pursuit, Control and Optimization. Wiley, New York (1965)
10. Kalandros, M., Pao, L.Y.: Covariance control for multisensor systems. IEEE Trans. Aerosp. Electron. Syst. **38**, 1138–1157 (2002)
11. Kreucher, C.M., Hero, A.O., Kastella, K.D., Morelande, M.R.: An information based approach to sensor management in large dynamic networks. IEEE Proc. **95**, 978–999 (2007)
12. Lane, M.H., Hoots, F.R.: General perturbations theories derived from the 1965 lane drag theory. Project Space Track Report No. 2, Aerospace Defense Command, Peterson AFB, CO (1979)
13. Li, X.R., Jilkov, V.P.: Survey of maneuvering target tracking. Part V, multiple-model methods. IEEE Trans. Aerosp. Electron. Syst. **41**, 1255–1321 (2005)
14. Pisacane, V.L., Mcconahy, R.J., Pryor, L.L., Whisnant, J.M., Black, H.D.: Orbit determination from passive range observations. IEEE Trans. Aerosp. Electron. Syst. **10**, 487–491 (1974)
15. Ru, J., Chen, H., Li, X.R., Chen, G.: A range rate based detection technique for tracking a maneuvering target. In: Proc. of SPIE Conf. Signal and Data Processing of Small Targets. San Diego, CA, USA (2005)

16. Teixeira, B.O.S., Santillo, M.A., Erwin, R.S., Bernstein, D.S.: Spacecraft tracking using sampled-data Kalman filters—an illustrative application of extended and unscented estimators. IEEE Control Syst. Mag. **28**(4), 78–94 (2008)
17. Vallado, D.A.: Fundamentals of Astrodynamics and Applications, 2nd edn. Microcosm Press, El Segundo (2001)
18. Van Trees, H.L.: Detection, Estimation, and Modulation Theory, Part I. Wiley, New York (1968)
19. Van Trees, H.L., Bell, K.L.: Bayesian Bounds for Parameter Estimation and Nonlinear Filtering/Tracking. Wiley-Interscience, New York (2007)
20. Zhao, Z., Li, X.R., Jilkov, V.P.: Best linear unbiased filtering with nonlinear measurements for target tracking. IEEE Trans. Aerosp. Electron. Syst. **40**, 1324–1336 (2004)